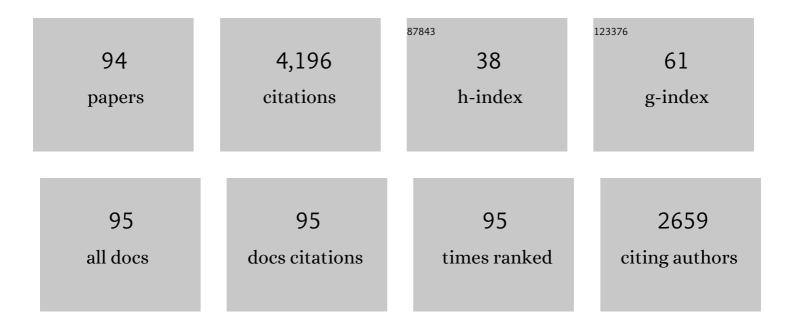
List of Publications by Year in descending order

Source: https://exaly.com/author-pdf/8072107/publications.pdf Version: 2024-02-01



KALLIWE HESS

#	Article	IF	CITATIONS
1	The effect of water on the viscosity of a haplogranitic melt under P-T-X conditions relevant to silicic volcanism. Contributions To Mineralogy and Petrology, 1996, 124, 19-28.	1.2	211
2	Non-Newtonian rheological law for highly crystalline dome lavas. Geology, 2007, 35, 843.	2.0	164
3	Seismogenic lavas and explosive eruption forecasting. Nature, 2008, 453, 507-510.	13.7	161
4	Viscosity, fragility, and configurational entropy of melts along the join SiO ₂ -NaAlSiO ₄ . American Mineralogist, 1997, 82, 979-990.	0.9	159
5	Universal representation of viscosity in glass forming liquids. Journal of Non-Crystalline Solids, 1998, 223, 207-222.	1.5	125
6	The influence of excess alkalis on the viscosity of a haplogranitic melt. American Mineralogist, 1995, 80, 297-304.	0.9	124
7	The influence of thermal-stressing (up to 1000°C) on the physical, mechanical, and chemical properties of siliceous-aggregate, high-strength concrete. Construction and Building Materials, 2013, 42, 248-265.	3.2	114
8	The viscous-brittle transition of crystal-bearing silicic melt: Direct observation of magma rupture and healing. Geology, 2012, 40, 611-614.	2.0	113
9	Volcanic ash melting under conditions relevant to ash turbine interactions. Nature Communications, 2016, 7, 10795.	5.8	113
10	Reconstructing magma failure and the degassing network of dome-building eruptions. Geology, 2013, 41, 515-518.	2.0	106
11	Rheological properties of dome lavas: Case study of Unzen volcano. Earth and Planetary Science Letters, 2009, 279, 263-272.	1.8	101
12	Volcanic sintering: Timescales of viscous densification and strength recovery. Geophysical Research Letters, 2013, 40, 5658-5664.	1.5	91
13	Extremely fluid behavior of hydrous peralkaline rhyolites. Earth and Planetary Science Letters, 1998, 158, 31-38.	1.8	85
14	Magmatic architecture of dome-building eruptions at Volcán de Colima, Mexico. Bulletin of Volcanology, 2012, 74, 249-260.	1.1	85
15	Thermal weakening of the carbonate basement under Mt. Etna volcano (Italy): Implications for volcano instability. Journal of Volcanology and Geothermal Research, 2013, 250, 42-60.	0.8	81
16	The viscosities of dry and hydrous XAlSi3O8 (X=Li, Na, K, Ca0.5, Mg0.5) melts. Chemical Geology, 2001, 174, 115-132.	1.4	77
17	A compositional tipping point governing the mobilization and eruption style of rhyolitic magma. Nature, 2017, 552, 235-238.	13.7	77
18	Tracking the permeable porous network during strain-dependent magmatic flow. Journal of Volcanology and Geothermal Research, 2013, 260, 117-126.	0.8	74

KAI-UWE HESS

#	Article	IF	CITATIONS
19	Nonisothermal viscous sintering of volcanic ash. Journal of Geophysical Research: Solid Earth, 2014, 119, 8792-8804.	1.4	71
20	Surface tension driven processes densify and retain permeability in magma and lava. Earth and Planetary Science Letters, 2016, 433, 116-124.	1.8	63
21	Parametrization of viscosity-temperature relations of aluminosilicate melts. Chemical Geology, 1996, 128, 155-163.	1.4	60
22	The rheology of peralkaline rhyolites from Pantelleria Island. Journal of Volcanology and Geothermal Research, 2013, 249, 201-216.	0.8	59
23	How tough is tuff in the event of fire?. Geology, 2012, 40, 311-314.	2.0	58
24	Melt viscosities in the system Na-Fe-Si-O-F-Cl; contrasting effects of F and Cl in alkaline melts. American Mineralogist, 1998, 83, 1016-1021.	0.9	57
25	Fusion characteristics of volcanic ash relevant to aviation hazards. Geophysical Research Letters, 2014, 41, 2326-2333.	1.5	57
26	The effect of oxygen fugacity on the rheological evolution of crystallizing basaltic melts. Earth and Planetary Science Letters, 2018, 487, 21-32.	1.8	57
27	XAS determination of the Fe local environment and oxidation state in phonolite glasses. American Mineralogist, 2011, 96, 631-636.	0.9	56
28	Approximate chemical analysis of volcanic glasses using Raman spectroscopy. Journal of Raman Spectroscopy, 2015, 46, 1235-1244.	1.2	53
29	Viscous flow behavior of tholeiitic and alkaline Fe-rich martian basalts. Geochimica Et Cosmochimica Acta, 2014, 124, 348-365.	1.6	48
30	Models for the estimation of Fe ³⁺ /Fe _{tot} ratio in terrestrial and extraterrestrial alkali- and iron-rich silicate glasses using Raman spectroscopyk. American Mineralogist, 2016, 101, 943-952.	0.9	48
31	Viscous heating in rhyolite: An in situ experimental determination. Earth and Planetary Science Letters, 2008, 275, 121-126.	1.8	46
32	Experimental generation of volcanic pseudotachylytes: Constraining rheology. Journal of Structural Geology, 2012, 38, 222-233.	1.0	46
33	Permeability of compacting porous lavas. Journal of Geophysical Research: Solid Earth, 2015, 120, 1605-1622.	1.4	46
34	Viscosity data for hydrous peraluminous granitic melts; comparison with a metaluminous model. American Mineralogist, 1998, 83, 236-239.	0.9	45
35	Wetting and Spreading of Molten Volcanic Ash in Jet Engines. Journal of Physical Chemistry Letters, 2017, 8, 1878-1884.	2.1	45
36	The rheological evolution of alkaline Vesuvius magmas and comparison with alkaline series from the Phlegrean Fields, Etna, Stromboli and Teide. Geochimica Et Cosmochimica Acta, 2009, 73, 6613-6630.	1.6	44

KAI-UWE HESS

#	Article	IF	CITATIONS
37	Effect of oxygen fugacity on the glass transition, viscosity and structure of silica- and iron-rich magmatic melts. Journal of Non-Crystalline Solids, 2017, 470, 78-85.	1.5	42
38	Granite and granitic pegmatite melts: volumes and viscosities. Earth and Environmental Science Transactions of the Royal Society of Edinburgh, 1996, 87, 65-72.	0.3	41
39	Topological inversions in coalescing granular media control fluid-flow regimes. Physical Review E, 2017, 96, 033113.	0.8	39
40	Combined effusive-explosive silicic volcanism straddles the multiphase viscous-to-brittle transition. Nature Communications, 2018, 9, 4696.	5.8	39
41	Shear Rateâ€Dependent Disequilibrium Rheology and Dynamics of Basalt Solidification. Geophysical Research Letters, 2018, 45, 6466-6475.	1.5	39
42	Synthesis, Crystal Structure, and Properties of Two Modifications of MgB12C2. Chemistry - A European Journal, 2007, 13, 3450-3458.	1.7	37
43	Spine growth and seismogenic faulting at Mt. Unzen, Japan. Journal of Geophysical Research: Solid Earth, 2015, 120, 4034-4054.	1.4	36
44	Centrifuge-assisted falling-sphere viscometry. European Journal of Mineralogy, 1996, 8, 507-514.	0.4	36
45	Viscous heating in silicate melts: An experimental and numerical comparison. Journal of Geophysical Research, 2012, 117, .	3.3	35
46	Estimation of CMAS infiltration depth in EB-PVD TBCs: A new constraint model supported with experimental approach. Journal of the European Ceramic Society, 2019, 39, 2936-2945.	2.8	35
47	Physical properties of the 1980 Mount St. Helens cryptodome magma. Bulletin of Volcanology, 1997, 59, 103-111.	1.1	34
48	Vesiculation and Quenching During Surtseyan Eruptions at Hunga Tongaâ€Hunga Ha'apai Volcano, Tonga. Journal of Geophysical Research: Solid Earth, 2018, 123, 3762-3779.	1.4	34
49	Experiments and models on H2O retrograde solubility in volcanic systems. American Mineralogist, 2015, 100, 774-786.	0.9	33
50	High-load, high-temperature deformation apparatus for synthetic and natural silicate melts. Review of Scientific Instruments, 2007, 78, 075102.	0.6	28
51	Shallow magmaâ€minglingâ€driven Strombolian eruptions at Mt. Yasur volcano, Vanuatu. Geophysical Research Letters, 2012, 39, .	1.5	27
52	Raman spectra of Martian glass analogues: A tool to approximate their chemical composition. Journal of Geophysical Research E: Planets, 2016, 121, 740-752.	1.5	27
53	Viscosity–temperature behaviour of dry melts in the Qz–Ab–Or system. Chemical Geology, 2001, 174, 133-142.	1.4	26
54	Modelling the non-Arrhenian rheology of silicate melts: Numerical considerations. European Journal of Mineralogy, 2002, 14, 417-428.	0.4	26

#	Article	IF	CITATIONS
55	Laboratory simulations of tensile fracture development in a volcanic conduit via cyclic magma pressurisation. Earth and Planetary Science Letters, 2012, 349-350, 231-239.	1.8	26
56	Synthesis, crystal growth and structure of Mg containing β-rhombohedral boron: MgB17.4. Journal of Solid State Chemistry, 2006, 179, 2900-2907.	1.4	25
57	Influence of cooling rate on thermoremanence of magnetite grains: Identifying the role of different magnetic domain states. Journal of Geophysical Research: Solid Earth, 2014, 119, 1599-1606.	1.4	25
58	Fault rheology beyond frictional melting. Proceedings of the National Academy of Sciences of the United States of America, 2015, 112, 9276-9280.	3.3	25
59	Synthesis and crystal structure of MgB12. Journal of Solid State Chemistry, 2006, 179, 2916-2926.	1.4	24
60	A cooling rate bias in paleointensity determination from volcanic glass: An experimental demonstration. Journal of Geophysical Research, 2010, 115, .	3.3	24
61	Volcanic edifice weakening via decarbonation: A selfâ€ŀimiting process?. Geophysical Research Letters, 2012, 39, .	1.5	24
62	Seismogenic frictional melting in the magmatic column. Solid Earth, 2014, 5, 199-208.	1.2	23
63	Eruptive shearing of tube pumice: pure and simple. Solid Earth, 2016, 7, 1383-1393.	1.2	22
64	Decarbonation and thermal microcracking under magmaticP-T-f CO2 conditions: the role of skarn substrata in promoting volcanic instability. Geophysical Journal International, 2013, 195, 369-380.	1.0	21
65	Synthesis and crystal structure of Mg2B24C, a new boron-rich boride related to "tetragonal boron l― Journal of Solid State Chemistry, 2006, 179, 2150-2157.	1.4	19
66	Cooling rates of lunar orange glass beads. Earth and Planetary Science Letters, 2018, 503, 88-94.	1.8	19
67	Enhancement of eruption explosivity by heterogeneous bubble nucleation triggered by magma mingling. Scientific Reports, 2017, 7, 16897.	1.6	18
68	Volcanic conduit failure as a trigger to magma fragmentation. Bulletin of Volcanology, 2012, 74, 11-13.	1.1	17
69	Magma mixing enhanced by bubble segregation. Solid Earth, 2015, 6, 1007-1023.	1.2	17
70	An advanced rotational rheometer system for extremely fluid liquids up to 1273 K and applications to alkali carbonate meltsk. American Mineralogist, 2016, 101, 953-959.	0.9	17
71	Advances in high-resolution neutron computed tomography: Adapted to the earth sciences. , 2011, 7, 1294-1302.		16
72	Reducing tool wear in abrasive cutting. International Journal of Machine Tools and Manufacture, 2005, 45, 1120-1123.	6.2	15

#	Article	IF	CITATIONS
73	Magma mixing induced by particle settling. Contributions To Mineralogy and Petrology, 2016, 171, 96.	1.2	15
74	The propagation and seismicity of dyke injection, new experimental evidence. Geophysical Research Letters, 2016, 43, 1876-1883.	1.5	14
75	Viscosities of granitic (sensu lato) melts: Influence of the anorthite component. American Mineralogist, 2000, 85, 1342-1348.	0.9	13
76	Paleointensities of phonolitic obsidian: Influence of emplacement rotations and devitrification. Journal of Geophysical Research, 2011, 116, .	3.3	13
77	<i>In situ</i> granulation by thermal stress during subaqueous volcanic eruptions. Geology, 2019, 47, 179-182.	2.0	12
78	Mineralogical and thermal characterization of a volcanic ash: Implications for turbine interaction. Journal of Volcanology and Geothermal Research, 2019, 377, 43-52.	0.8	12
79	Variability in composition and physical properties of the sedimentary basement of Mt Etna, Italy. Journal of Volcanology and Geothermal Research, 2015, 302, 102-116.	0.8	11
80	Aggregation in particle rich environments: a textural study of examples from volcanic eruptions, meteorite impacts, and fluidized bed processing. Bulletin of Volcanology, 2018, 80, 32.	1.1	11
81	Eruption and emplacement timescales of ignimbrite super-eruptions from thermo-kinetics of glass shards. Frontiers in Earth Science, 2015, 3, .	0.8	10
82	The roles of microlites and phenocrysts during degassing of silicic magma. Earth and Planetary Science Letters, 2022, 577, 117264.	1.8	10
83	Paleointensities on 8 ka obsidian from Mayor Island, New Zealand. Solid Earth, 2011, 2, 259-270.	1.2	9
84	Paleointensity on volcanic glass of varying hydration states. Physics of the Earth and Planetary Interiors, 2012, 208-209, 25-37.	0.7	9
85	Vesiculation in rhyolite at low <scp>H</scp> ₂ <scp>O</scp> contents: A thermodynamic model. Geochemistry, Geophysics, Geosystems, 2015, 16, 4292-4310.	1.0	9
86	Determination of the hydrogen-bond network and the ferrimagnetic structure of a rockbridgeite-type compound, \${{m Fe^{2+}Fe^{3+}_{3.2}(Mn^{2+}, Zn)_{0.8}(PO_{4})_{3}(OH)_{4.2}(HOH)_{0.8}}}\$. Journal of Physics Condensed Matter, 2018, 30, 235401.	0.7	8
87	Local geology controlled the feasibility of vitrifying Iron Age buildings. Scientific Reports, 2017, 7, 40028.	1.6	7
88	Intrinsic proton dynamics in hydrous silicate melts as seen by quasielastic neutron scattering at elevated temperature and pressure. Chemical Geology, 2017, 461, 152-159.	1.4	5
89	The glass transition and the non-Arrhenian viscosity of carbonate melts. American Mineralogist, 2022, 107, 1053-1064.	0.9	5
90	Determination of water speciation in hydrous haplogranitic glasses with partial Raman spectra. Chemical Geology, 2020, 553, 119793.	1.4	4

#	Article	IF	CITATIONS
91	A model for the kinetics of high-temperature reactions between polydisperse volcanic ash and SO2 gas. American Mineralogist, 2021, 106, 1319-1332.	0.9	4
92	The feasibility of vitrifying a sandstone enclosure in the British Iron Age. Journal of Archaeological Science: Reports, 2015, 4, 605-612.	0.2	2
93	Volcanic glass and its suitability to recover the ancient geomagnetic field strength. Geological Society Special Publication, 2015, 396, 265-276.	0.8	1
94	Using obsidian in glass art practice. Volcanica, 2022, 5, 183-207.	0.6	1